
AN EMPIRICAL STUDY OF THE EFFECT OF BACKGROUND DATA SIZE ON THE STABILITY OF SHAPLEY ADDITIVE EXPLANATIONS (SHAP) FOR DEEP LEARNING MODELS

Han Yuan*
yuan.han.ai@outlook.com

Mingxuan Liu*
mingxuan99michelle@gmail.com

Michael Krauthammer
michael.krauthammer@uzh.ch

Lican Kang
kanglican@whu.edu.cn

Chenkui Miao
miaochenkui@njmu.edu.cn

Ying Wu
ywu@nankai.edu.cn

ABSTRACT

Nowadays, the interpretation of why a machine learning (ML) model makes certain inferences is as crucial as the accuracy of such inferences. Some ML models like the decision tree possess inherent interpretability that can be directly comprehended by humans. Others like artificial neural networks (ANN), however, rely on external methods to uncover the deduction mechanism. SHapley Additive exPlanations (SHAP) is one of such external methods, which requires a background dataset when interpreting ANNs. Generally, a background dataset consists of instances randomly sampled from the training dataset. However, the sampling size and its effect on SHAP remain to be unexplored. In our empirical study on the MIMIC-III dataset, we show that the two core explanations - SHAP values and variable rankings fluctuate when using different background datasets acquired from random sampling, indicating that users cannot unquestioningly trust the one-shot interpretation from SHAP. Luckily, such fluctuation decreases with increase of the background dataset size. Also, we notice an U-shape in the stability assessment of SHAP variable rankings, demonstrating that SHAP is more reliable in ranking the most and least important variables compared to moderately important ones. Overall, our results suggest that users should take into account how background data affects SHAP results, with improved SHAP stability as the background sample size increases.

Keywords Interpretable Machine Learning · SHapley Additive exPlanations (SHAP) · Background Data

1 Introduction

With the surging deployment of machine learning (ML) models on real-world tasks [1, 2, 3, 4], tools for interpreting model inference are becoming as important as techniques for enhancing model accuracy [5, 6]. Some ML models like the decision tree are intrinsically explainable and easily understood by humans. Other ML models, particularly those based on artificial neural networks (ANNs), are too complex to be interpreted even by experts [7]. To address this problem, researchers proposed various post-hoc explanation methods and added them extrinsically to these complex models without altering their inner architectures. There are two levels in the post-hoc explanations: instance-level and model-level. While instance-level explanation typically provides feature contribution analyses for a single prediction, model-level explanation provides feature importance across all predictions made by a ML model.

SHapley Additive exPlanations (SHAP) [7] provides both instance-level and model-level explanations through SHAP values and variable rankings respectively. SHAP values are the direct production from SHAP calculations while variable rankings are acquired by comparing the sum of each variable's absolute SHAP values across all instances [8]. To eliminate computing complexity, the SHAP package [7] includes various explainers for different ML models. DeepExplainer is such an efficient explainer for ANNs and requires a background dataset to serve as a prior expectation towards the instances to be explained.

*Equal contribution

While the official SHAP documentation ² suggests 100 randomly drawn samples from the training data as an adequate background dataset, other studies employed different sampling sizes [9, 10, 11]. This raises an important question: What is the effect of different background dataset sizes on SHAP explanations of ANNs? In a pilot experiment, we found that both instance-level SHAP values and model-level variable rankings fluctuate when we adopt small-size random sampling to obtain background datasets. To quantify such fluctuation and better answer the question above, we conducted an empirical study with different background dataset sizes applied to a three-layer ANN and MIMIC-III [12] data. We then directly quantified the effect on instance-level explanations (SHAP values) and used an exact (BLEU score [13]) and fuzzy (Jaccard index [14]) approach for evaluating model-level explanations (variable rankings).

2 Method

2.1 SHAP values and variable rankings

SHAP provides instance-level and model-level explanations by SHAP value and variable ranking, respectively. In a binary classification task (label is 0 or 1), the inputs of an ANN model are variables $var_{i,j}$ from an instance D_i and the output is the prediction probability P_i of D_i of being classified as label 1. In general, we are interested in interpreting a stack of instances D at both the instance and model-level.

$$D = \{D_i\}, i = 1, \dots, N \quad (1)$$

$$D_i = \{var_{i,j}\}, j = 1, \dots, V \quad (2)$$

$$P_i = ANN(D_i), i = 1, \dots, N \quad (3)$$

where i represents the i -th instance in D and j stands for the j -th variable in D_i .

DeepExplainer, the function for SHAP calculations in an ANN, provides instance-level explanations of P_i through the contribution ($shap_{i,j,bg}$) of each variable ($var_{i,j}$) to the prediction deviation from a prior P_{bg} , which is the probability expectation of samples in the background dataset bg .

$$P_i - P_{bg} = \sum_{j=1}^V shap_{i,j,bg} \quad (4)$$

With the instance-level $shap_{i,j,bg}$, we then compute the model-level variable importance $I_{j,bg}$ [7] as follows:

$$I_{j,bg} = \sum_{i=1}^N |shap_{i,j,bg}| \quad (5)$$

where absolute SHAP values for a particular variable are summed over all instances in D . Based on variable importance, users obtain the variable rankings effortlessly (larger $I_{j,bg}$, higher importance and ranking).

As shown in formula 4 and 5, a background dataset is a prerequisite for DeepExplainer and its application on ANNs interpretation. Generally, a background dataset consists of instances randomly sampled from the training data [7]. However, the use of small background sample sizes potentially causes fluctuation of SHAP explanations, which may affect users' trust in the one-shot SHAP explanations.

While statistical variance is well suited for evaluating the fluctuations of SHAP values, we need more refined measures for assessing changes in variable rankings. Specifically, as changes in variable rankings can be seen as equivalent to words order changes, we adopt the BLEU assessment, typically used to compare the word order of a translated text with regard to a reference translation, for measuring differences in variable rankings. Another potential evaluation comes from similarity computation in set theory: the Jaccard index.

2.2 Fluctuation quantification of variable ranking

2.2.1 BLEU for exact fluctuation evaluations

BLEU [13] aims for evaluating machine translation through comparing n-gram matches between the candidate translation and the reference translation. An n-gram is a contiguous sequence of n items from a given text. The first step in BLEU is to compute the n-gram matches precision score p_n : the matched n-gram counts in the candidate translation

²SHAP documentation, available from <https://shap.readthedocs.io/en/latest>

over the number of candidate n-grams in the reference translation. The second step is to multiply $p_n^{\frac{1}{2^n}}$ ($1 \leq n \leq k$, n is an integer) with penalty terms: $\exp(\min(0, 1 - \frac{l_c}{l_r}))$, where k is the maximum number of words in the matched subsequence, and l_c and l_r stand for lengths of the candidate translation and the reference translation respectively.

$$\text{BLEU} = \exp \left(\min \left(0, 1 - \frac{l_c}{l_r} \right) \right) \prod_{n=1}^k p_n^{\frac{1}{2^n}} \quad (6)$$

As stated above, if we treat one variable ranking as “the candidate translation” and the other as “the reference translation”, we can also compute the difference between these two rankings. The formula 6 is modified to suit our application: (1) Since the ranking sequences are of equal length and contain the same elements, the $\exp(\min(0, 1 - \frac{l_c}{l_r}))$ and p_1 are always 1; (2) Only two-grams BLEU is used to quantify the relevant sequence between two rankings; (3) Considering that two-grams BLEU might fail to detect the drastic order change of two-grams units, we proposed quartile-based computation where the variable ranking is split into four quartiles, $p_{2,q}^{\frac{1}{4}}$ is calculated for each quartile q ($q = 1, 2, 3, 4$), and the average value BLEU_Q serves as the final assessment value.

$$\text{BLEU}_Q = \frac{1}{4} \times \sum_{q=1}^4 p_{2,q}^{\frac{1}{4}} \quad (7)$$

We use a fictive example to clarify BLEU_Q (See Table 1). There are two rankings: Ranking #1 [a, b, c, d, e, f, g, h, i, j, k, l] and Ranking #2 [a, c, b, d, e, f, h, g, i, j, k, l]. We first split the two rankings into four parts. For example, Ranking #1 is split into [a, b, c], [d, e, f], [g, h, i], and [j, k, l]. Then we calculate two-grams in each quartile of these two rankings. Ranking #1's first part is [a, b, c] and corresponding two-grams are [a, b] and [b, c]. With two-grams in each quartile, we can easily obtain the matched two-grams counts and the number of two-grams. Finally, the BLEU_Q here is $\frac{1}{4} \times (0^{\frac{1}{4}} + 1^{\frac{1}{4}} + 0^{\frac{1}{4}} + 1^{\frac{1}{4}}) = 0.25$ according to formula 7.

Table 1: Two-grams and the corresponding precision score of Ranking #1 and #2

Quartile	Ranking #1	Ranking #2	Matched Num	Reference Num	Precision Score
0-25%	[a, b], [b, c]	[a, c], [c, b]	0	2	0/2 = 0
25-50%	[d, e], [e, f]	[d, e], [e, f]	2	2	2/2 = 1
50-75%	[g, h], [h, i]	[h, g], [g, i]	0	2	0/2 = 0
75-100%	[j, k], [k, l]	[j, k], [k, l]	2	2	2/2 = 1

“Matched Num” means the number of matched two-gram units between two variable rankings in each quartile.

“Reference Num” refers to the number of two-gram units in one variable ranking in each quartile.

2.2.2 Jaccard index for fuzzy fluctuation evaluations

In contrast to BLEU_Q which focuses on the exact match of two-gram units, Jaccard index [14], defined as the size of the intersection divided by the size of the union of the sample sets, is used for evaluating the fuzzy similarity between sample sets. Given that any ranking in our study contains the same variables, the Jaccard index cannot be directly used.

Like BLEU_Q , we propose the quartile-based Jaccard_Q , wherein the variable ranking is split into four quartiles, Jaccard_q is calculated in each quartile q ($q = 1, 2, 3, 4$), and the average value across all quartiles works as a final assessment of the fluctuation of variable rankings.

$$\text{Jaccard}_Q = \frac{1}{4} \times \sum_{q=1}^4 \text{Jaccard}_q \quad (8)$$

The same fictive sample is used for clarification (See Table 2): We first split the two rankings into four parts, then compute the intersection, union number, and Jaccard index in each quartile, and finally obtain the mean value of all Jaccard indexes $\frac{1}{4} \times (1 + 1 + 1 + 1) = 1$.

2.3 Study design

2.3.1 Dataset

We implemented an empirical study of SHAP stability using the same de-identified intensive care unit dataset as our previous paper [15]. This dataset includes 44,918 admission episodes (including 3,958 positive episodes, defined as

Table 2: Variable subsets and corresponding Jaccard index of Ranking #1 and #2

Quartile	Ranking #1	Ranking #2	Intersection Num	Union Num	Jaccard index
0-25%	a, b, c	a, c, b	3	3	3/3 = 1
25-50%	d, e, f	d, e, f	3	3	3/3 = 1
50-75%	g, h, i	h, g, i	3	3	3/3 = 1
75-100%	j, k, l	j, k, l	3	3	3/3 = 1

“Intersection Num” means the number of variables in the intersection between these two rankings in each quartile.

“Union Num” refers to the number of variables in the union between the two rankings in each quartile.

admissions within patient mortality) of the Beth Israel Deaconess Medical Center between 2001 and 2012 (MIMIC-III dataset) [12].

We randomly separated the data set into development and explanation sets. The development set consisted of 31,442 (70%) patients, and the explanation set was made up of 13,476 (30%) patients. The development set was used to develop the ANN and to generate background datasets. The explanation set was put aside to be interpreted by SHAP.

The variables to be ranked included temperature, heart rate, age, respiration rate, systolic blood pressure, diastolic blood pressure, mean arterial pressure, peripheral capillary oxygen saturation (SpO2), white blood cell count, platelet count, anion gap, glucose, sodium, potassium, lactate, bicarbonate, blood urea nitrogen, creatinine, hemoglobin, chloride, and hematocrit.

2.3.2 Model architecture

An ANN with three layers was used as backbone model in this study because no substantial gain was observed with more layers. The ANN was made up with 2 hidden layers with 128 and 64 rectified linear units respectively and 1 output layer using sigmoid activation.

2.3.3 Empirical study setting

We varied background data size from 100 to 1,000 and performed 100 simulations under each background data size. In each simulation, a background dataset with a fixed size was sampled from the training dataset. Then SHAP values and variable rankings are calculated on the explanation set. After 100 simulations, we obtained 100 SHAP values for each variable in a single instance and applied statistical variance to depict the fluctuation of SHAP values in this instance: For variable var_j , its variance sum is $\sum_{i=1}^N \frac{1}{99} \sum_{bg=1}^{100} (|shap_{i,j,bg}| - \frac{1}{100} \sum_{bg=1}^{100} |shap_{i,j,bg}|)^2$. Also, we received $p = 100$ variable rankings and C_p^2 different pairs of rankings in the model-level. BLEU_Q^k and Jaccard_Q^k represents the quartile-based BLEU_Q and Jaccard_Q index of the k -th pair, respectively. Then the mean of BLEU_Q^k and Jaccard_Q^k across all pairs were calculated to assess the fluctuation of variable rankings.

$$\text{Mean BLEU} = \sum_{k=1}^{C_p^2} (\text{BLEU}_Q^k) \quad (9)$$

$$\text{Mean Jaccard} = \sum_{k=1}^{C_p^2} (\text{Jaccard}_Q^k) \quad (10)$$

All computations were carried out using PyTorch version 1.6.0, Python version 3.8, and R version 4.0.3. The source code is available at GitHub³.

3 Results

Using MIMIC-III data, we evaluated the impact of the background dataset size on both instance-level and model-level SHAP explanations. The fluctuation of instance-level SHAP values was assessed using statistical variance, while the instability of model-level variable rankings was evaluated using the proposed Mean BLEU and Mean Jaccard measures.

³Source code, available from <https://github.com/Han-Yuan-Med/SHAP-Robustness>

3.1 Fluctuation of SHAP values

The fluctuation of instance-level SHAP explanations originates from changes of SHAP values, as assessed by a statistical variance measure. We observe that the variance sum per variable across instances in the explanation set decreases as the background sample size increases (Table 3).

Table 3: The mean variance of SHAP values across all observations

Variables	Variance sum (m=100)	Variance sum (m=300)	Variance sum (m=500)	Variance sum (m=1000)
Age	153.31	34.34	22.16	11.21
Heart rate	26.71	13.38	8.85	5.20
Systolic blood pressure	271.31	78.28	44.27	24.13
Diastolic blood pressure	74.64	15.88	11.22	5.52
Arterial pressure	169.92	36.78	22.91	13.32
Respiration rate	33.08	7.87	5.75	2.85
Temperature	0.50	0.17	0.10	0.05
SpO2	1.70	0.51	0.21	0.13
Glucose	72.18	31.77	16.35	7.32
Anion gap	5.64	2.59	1.54	0.77
Bicarbonate	10.17	3.16	2.02	1.11
Creatinine	56.95	15.15	7.92	3.82
Chloride	67.52	11.69	7.85	3.17
Lactate	22.63	11.64	6.93	3.05
Hemoglobin	1.56	0.31	0.18	0.10
Hematocrit	3.58	0.64	0.35	0.18
Platelet	325.33	75.95	49.46	23.21
Potassium	3.71	1.38	0.86	0.47
Blood urea nitrogen	212.63	54.12	30.46	15.60
Sodium	60.20	9.66	6.54	2.65
White blood cells	83.88	21.96	10.40	5.71

“m” represents the sample size of the background dataset.

3.2 Fluctuation of variable rankings

Fluctuation of instance-level SHAP values may also indicate unstable model-level variable rankings. Figure 1 visualizes the simulation results with background dataset sizes of 100 and 1,000, respectively. We observe more stable rankings with the larger dataset.

Though better stability was observed in larger background data, quantitative assessment is still necessary for accurate analyses. We utilized the quartile-based BLEU and Jaccard index to quantify the exact and fuzzy stabilities. Tables 4 and 5 demonstrate that the pairwise analyses of the different rankings resulted in improved BLEU and Jaccard scores when the background dataset size increased. While the Jaccard index was close to 0.9 across all four quartiles, the BLEU results indicate that the relevant variable orders fluctuate even using many background samples, with a score of 0.644 for 1000 background samples. Interestingly, the BLEU and Jaccard index values showed a U-shape indicating higher stabilities in Quartiles 1 and 4 compared to Quartiles 2 and 3.

Table 4: Quartile-based BLEU results

m	Average	Quartile 1	Quartile 2	Quartile 3	Quartile 4
100	0.432	0.478	0.269	0.360	0.619
200	0.464	0.521	0.313	0.380	0.643
300	0.510	0.574	0.348	0.446	0.674
400	0.545	0.605	0.366	0.488	0.722
500	0.557	0.594	0.387	0.509	0.739
1000	0.644	0.657	0.476	0.624	0.818

“m” represents the sample size of the background dataset.

“Average” stands for the Mean BLEU across four quartiles, see formula 9.

Table 5: Quartile-based Jaccard index results

m	Average	Quartile 1	Quartile 2	Quartile 3	Quartile 4
100	0.432	0.478	0.269	0.360	0.619
200	0.464	0.521	0.313	0.380	0.643
300	0.510	0.574	0.348	0.446	0.674
400	0.545	0.605	0.366	0.488	0.722
500	0.557	0.594	0.387	0.509	0.739
1000	0.644	0.657	0.476	0.624	0.818

“m” represents the sample size of the background dataset.

“Average” stands for the Mean Jaccard across four quartiles, see formula 10.

4 Discussion

The potential to provide robust explanations is an important desiderata for an explanation tool [16]. Our empirical study quantifies the stability of SHAP explanations at both the instance (SHAP values) and model-level (variable rankings).

Our results point to a positive relationship between background sample size and the stability of SHAP explanations. More coherent SHAP values and variable rankings were observed when larger background datasets were used. This phenomenon could be partially explained by an inference of the central limit theorem: The background dataset converges to the overall distribution at the standard rate of the root of sample size [17, 18]. Therefore, sampling with a larger size could lead to less randomness, generation of a more representative background dataset, and more stable SHAP explanations. Furthermore, our results suggested that the optimal background dataset size depends on a user’s expectation with regard to the exactness of the ranking. For example, in our pairwise analysis using the BLEU score, we did not observe exact replicate variable order rankings, even at large background data sizes. On the other hand, we saw stable rankings using a fuzzy ranking comparison (Jaccard index), even at small background dataset sizes. Therefore, while SHAP is a trustworthy method for evaluating variable importance, the concrete variable importance ranking requires careful consideration. Particularly, the U-shape of the comparative BLEU and Jaccard scores indicate that SHAP is more reliable in ranking the most and least important variables compared to the moderately important ones.

The results suggest that SHAP users should use a background dataset as large as possible, and could even consider to use the whole training dataset as a background dataset. However, larger background datasets lead to more expensive computation and the computing budget is limited for most researchers. To estimate the upper limit of an affordable background sample size, we recommend that SHAP users conduct a pilot experiment using a small background dataset (size of 100, for example) to estimate the computational complexity. Given a complexity C_{100} derived from background dataset with 100 samples, the complexity C_m using background dataset with m samples can be approximated by $\frac{m}{100} \times C_{100}$ because of the linear relationship between background sample size and computational complexity [7]. Once a decision on the size of the background dataset has been reached, users should make sure that the background dataset is representative for the complete dataset. To this end, some researchers recommend sampling from high-density areas [19] or using K-means clustering [20].

There are several limitations to this study. First, it was based on one dataset and one ANN model. Additional studies using various datasets and diverse ANN models can further validate the results. Second, only 100 simulations were performed in each scenario and future work should include larger simulations. Last, although our study uncovered a stability issue in SHAP explanations and pointed out that large background sample sizes mitigate the issue, a formal rule

for determining the optimal background dataset size is still lacking. Further research involving established sampling theories could aid in this regard.

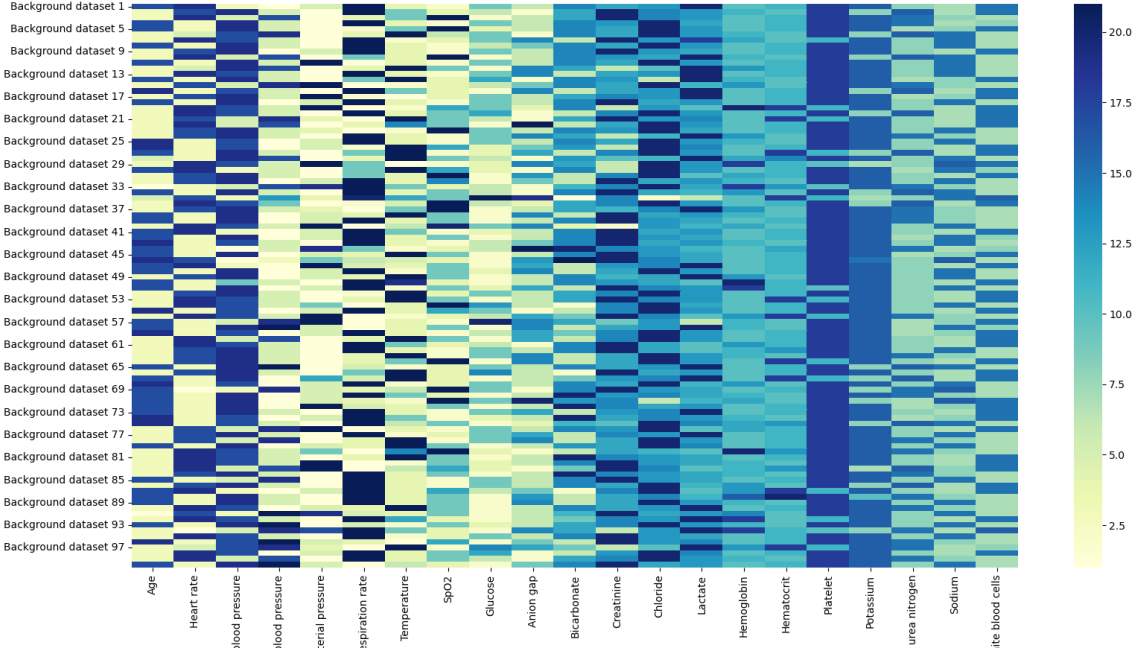
5 Conclusion

Through an empirical study, we have shown that SHAP explanations fluctuate when using a small background sample size and that these fluctuations decrease when the background dataset sampling size increases. This finding holds true for both instance and model-level explanations. Using the BLEU score and Jaccard index for assessing the stability of the model-level variable rankings, we observe an U-shape of the respective measures, which is indicative that SHAP is more reliable in ranking the most and least important variables compared with the moderately important ones. Overall, our results suggest that the stability problem caused by the choice of the background dataset size should not be ignored by SHAP users and that users should opt for larger dataset sizes to mitigate fluctuations in SHAP explanations.

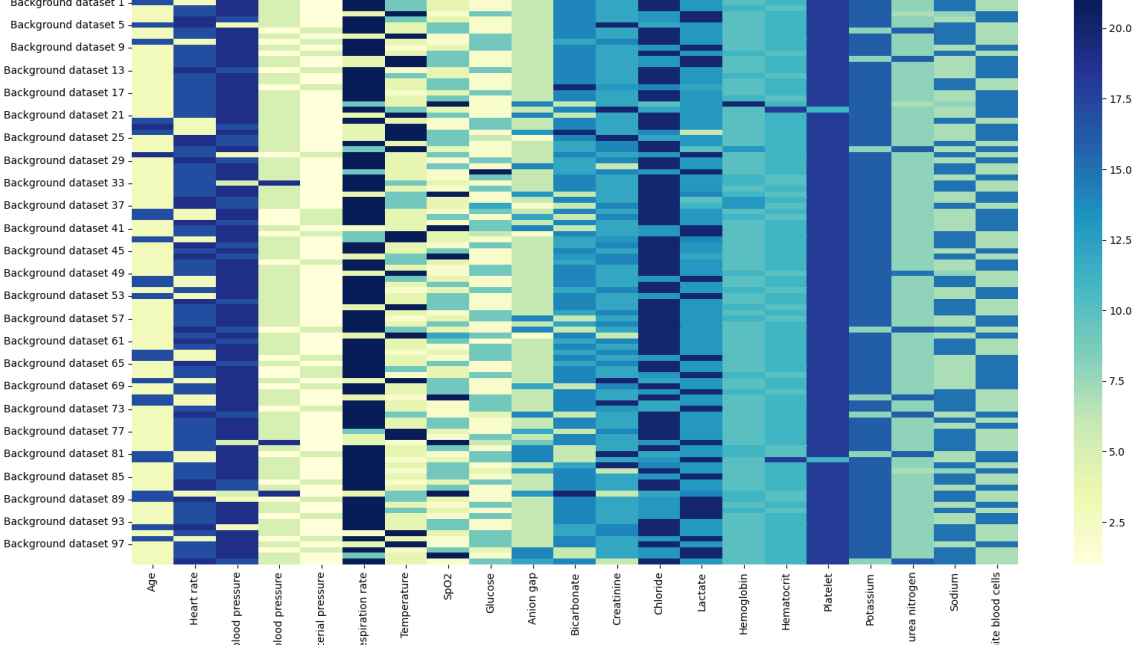
References

- [1] Suman Ravuri, Karel Lenc, Matthew Willson, Dmitry Kangin, Remi Lam, Piotr Mirowski, Megan Fitzsimons, Maria Athanassiadou, Sheleem Kashem, Sam Madge, et al. Skilful precipitation nowcasting using deep generative models of radar. *Nature*, 597(7878):672–677, 2021.
- [2] John Jumper, Richard Evans, Alexander Pritzel, Tim Green, Michael Figurnov, Olaf Ronneberger, Kathryn Tunyasuvunakool, Russ Bates, Augustin Žídek, Anna Potapenko, et al. Highly accurate protein structure prediction with alphafold. *Nature*, 596(7873):583–589, 2021.
- [3] Oriol Vinyals, Igor Babuschkin, Wojciech M Czarnecki, Michaël Mathieu, Andrew Dudzik, Junyoung Chung, David H Choi, Richard Powell, Timo Ewalds, Petko Georgiev, et al. Grandmaster level in starcraft ii using multi-agent reinforcement learning. *Nature*, 575(7782):350–354, 2019.
- [4] Yi Xin Zhao, Han Yuan, and Ying Wu. Prediction of adverse drug reaction using machine learning and deep learning based on an imbalanced electronic medical records dataset. In *2021 5th International Conference on Medical and Health Informatics*, page 17–21, 2021.
- [5] Simon Meyer Lauritsen, Mads Kristensen, Mathias Vassard Olsen, Morten Skaarup Larsen, Katrine Meyer Lauritsen, Marianne Johansson Jørgensen, Jeppe Lange, and Bo Thiesson. Explainable artificial intelligence model to predict acute critical illness from electronic health records. *Nature communications*, 11(1):1–11, 2020.
- [6] Feng Xie, Han Yuan, Yilin Ning, Marcus Eng Hock Ong, Mengling Feng, Wynne Hsu, Bibhas Chakraborty, and Nan Liu. Deep learning for temporal data representation in electronic health records: A systematic review of challenges and methodologies. *Journal of Biomedical Informatics*, 126:103980, 2022.
- [7] Scott M Lundberg and Su-In Lee. A unified approach to interpreting model predictions. In I. Guyon, U. Von Luxburg, S. Bengio, H. Wallach, R. Fergus, S. Vishwanathan, and R. Garnett, editors, *Advances in Neural Information Processing Systems*, volume 30, 2017.
- [8] Scott M Lundberg, Gabriel Erion, Hugh Chen, Alex DeGrave, Jordan M Prutkin, Bala Nair, Ronit Katz, Jonathan Himmelfarb, Nisha Bansal, and Su-In Lee. From local explanations to global understanding with explainable ai for trees. *Nature machine intelligence*, 2(1):56–67, 2020.
- [9] Bas HM van der Velden, Markus HA Janse, Max AA Ragusi, Claudette E Loo, and Kenneth GA Gilhuijs. Volumetric breast density estimation on mri using explainable deep learning regression. *Scientific Reports*, 10(1):1–9, 2020.
- [10] Sven H Giese, Ludwig R Sinn, Fritz Wegner, and Juri Rappaport. Retention time prediction using neural networks increases identifications in crosslinking mass spectrometry. *Nature communications*, 12(1):1–11, 2021.
- [11] Kevin Kaufmann, Hobson Lane, Xiao Liu, and Kenneth S Vecchio. Efficient few-shot machine learning for classification of ebsd patterns. *Scientific reports*, 11(1):1–12, 2021.
- [12] Alistair EW Johnson, Tom J Pollard, Lu Shen, Li-wei H Lehman, Mengling Feng, Mohammad Ghassemi, Benjamin Moody, Peter Szolovits, Leo Anthony Celi, and Roger G Mark. Mimic-iii, a freely accessible critical care database. *Scientific data*, 3(1):1–9, 2016.
- [13] Kishore Papineni, Salim Roukos, Todd Ward, and Wei-Jing Zhu. Bleu: a method for automatic evaluation of machine translation. In *Proceedings of the 40th annual meeting of the Association for Computational Linguistics*, pages 311–318, 2002.
- [14] Sam Fletcher and Md Zahidul Islam. Comparing sets of patterns with the jaccard index. *Australasian Journal of Information Systems*, 22, Mar. 2018.

- [15] Han Yuan, Feng Xie, Marcus Eng Hock Ong, Yilin Ning, Marcel Lucas Chee, Seyed Ehsan Saffari, Hairil Rizal Abdullah, Benjamin Alan Goldstein, Bibhas Chakraborty, and Nan Liu. Autoscore-imbalance: An interpretable machine learning tool for development of clinical scores with rare events data. *Journal of Biomedical Informatics*, 129:104072, 2022.
- [16] Himabindu Lakkaraju, Nino Arsov, and Osbert Bastani. Robust and stable black box explanations. In Hal Daumé III and Aarti Singh, editors, *Proceedings of the 37th International Conference on Machine Learning*, volume 119 of *Proceedings of Machine Learning Research*, pages 5628–5638, 2020.
- [17] Murray Rosenblatt. A central limit theorem and a strong mixing condition. *Proceedings of the National Academy of Sciences of the United States of America*, 42(1):43, 1956.
- [18] Xinran Li and Peng Ding. General forms of finite population central limit theorems with applications to causal inference. *Journal of the American Statistical Association*, 112(520):1759–1769, 2017.
- [19] Been Kim, Rajiv Khanna, and Oluwasanmi O Koyejo. Examples are not enough, learn to criticize! criticism for interpretability. In D. Lee, M. Sugiyama, U. Luxburg, I. Guyon, and R. Garnett, editors, *Advances in Neural Information Processing Systems*, volume 29, 2016.
- [20] Yuki Oba, Taro Tezuka, Masaru Sanuki, and Yukiko Wagatsuma. Interpretable prediction of diabetes from tabular health screening records using an attentional neural network. In *2021 IEEE 8th International Conference on Data Science and Advanced Analytics (DSAA)*, pages 1–11, 2021.



(a) The variable rankings using 100 background dataset samples.



(b) The variable rankings using 1,000 background dataset samples.

Figure 1: Fluctuation of variable rankings using background size of 100 and 1,000. Based on 100 simulations, we obtained 100 variable rankings for each of the two background sizes. Each row corresponds to one simulation; each column represents a variable's ranking order across the 100 simulations. The color bar on the right indicates the variable ranking sequence (blue means low rankings and yellow stands for high rankings). The small color blocks in each column of sub-figure (b) change less than these of (a), indicating that smaller volatilities appear with background size 1,000.